

### **Author response to review 1:**

We thank the referee for his careful review of the manuscript and the many useful suggestions and constructive comments, which helped us to improve the manuscript. In the following, we discuss these comments and document the associated changes we applied to our manuscript.

### **Anonymous Referee #1 Received and published: 8 December 2019**

**Comment:** Please provide the data used for the manuscript in a data repository, or at least as supplementary material

**Author response:** The data is available in github in the following repository:  
[https://github.com/rockphysicsUNIL/GDPI\\_Well\\_log\\_data](https://github.com/rockphysicsUNIL/GDPI_Well_log_data)

**Comment 1:** The manuscript is pleasant to read, although some paragraphs in the "results section" better fit in a "discussion section". However, I found the the discussion part a bit light.

**Author response:** The discussion section in the manuscript was indeed a bit light, since part of it was accidentally commented out in the tex file before conversion to pdf. We apologize for this.

**Changes in the manuscript:** This "missing" part of the discussion has been added in the updated manuscript and is attached at the end of the document.

**Comment 2:** What are the implications of this fracture network for the system? maybe as far as petrothermal reservoirs and exploitable natural hydrothermal systems, as mentioned in the abstract and in the introduction? In the discussion part the authors do not discuss the implications of their study, in particular the importance of the results on the fluid flow in/out of the borehole.

**Author response and changes in the manuscript:** The last paragraph of the discussion section now addresses the implications of the fracture network with respect to the flow system and potential exploitable reservoirs in conjunction with published works of Egli et. (2018) and Wanner et al. (2019). However, we do not feel that conclusions can be drawn solely on the basis of the information obtained from the logging data.

**Comment 3.** The authors used the electrical resistivity. But it is not clear if they performed this measurement with the dual laterolog (DLL) or another tool? If so please add in the figure both resistivity curves DLL depth and DLLshallow and their ratio or explain why they are not used. This measurement can help to distinguish the invade fluid zones.

**Author response:** The measurements are not performed with a dual laterolog tool. The utilized tool is an older-generation slimhole logging tool, which performs normal resistivity measurements. Figure 5 in the manuscript shows 4 resistivity curves corresponding to spacings of 8, 16, 32 and 64 inch between the current electrode A and potential electrode M. The spacing between the electrodes may serve as a first-order approximation of the expected penetration depth.

The utilized electrical resistivity measurements were performed in 2016, a year after drilling was completed, and, thus, we assume that the borehole and formation fluids are in equilibrium and that overall the system is in its "natural state". Thus, there should not be any invaded fluid zones. The 2015 data, which are not used in this study, are complicated by the fact that, after the drilling with polymer mud, the borehole was flushed several times with lake water over a period of days to enable optical televiewer measurements. This happened before the resistivity measurements were performed. Figure B1 in the Appendix of the manuscript illustrates the difference between the 2015 and 2016 data for the 16" norm. resistivity measurement. The logs show a very good match with regard to their overall behavior; however, their absolute values differ in the upper part of the borehole. The difference decreases towards the bottom of the borehole.

Nevertheless, the shallow resistivity measurements (8") show lower values in the zones of severe borehole enlargements than the deeper ones for all data sets. This is probably purely an effect of the enlarged borehole diameter. Corrections to remove the effect of borehole enlargements have been trialed in the scope of a master project, but they did not lead to improved results of the resistivity data.

**Changes in the manuscript:** We added in Table 1 that the tool measures normal resistivity.

**Comment 4.** The authors mentioned often in the manuscript the aperture of the fractures to support their interpretation. Unfortunately, no table or plot with this information are present in the manuscript. I suggest the author to add a table to list the number of fractures, their geometry (strike, dip) and the aperture.

**Author response and changes in the manuscript:** The aperture is shown together with the SP data in Figure 11 and the dip and azimuth are shown as polar plots together with the borehole radar data in Figure 2. However, we agree with the referee that this information is rather hidden. Therefore, the following figure showing the aperture of the fractures, their relative azimuth (strike) and dip with respect to the borehole trajectory has been added to the manuscript. A text file which lists the fractures and their properties is available on [https://github.com/rockphysicsUNIL/GDPI\\_Well\\_log\\_data](https://github.com/rockphysicsUNIL/GDPI_Well_log_data).

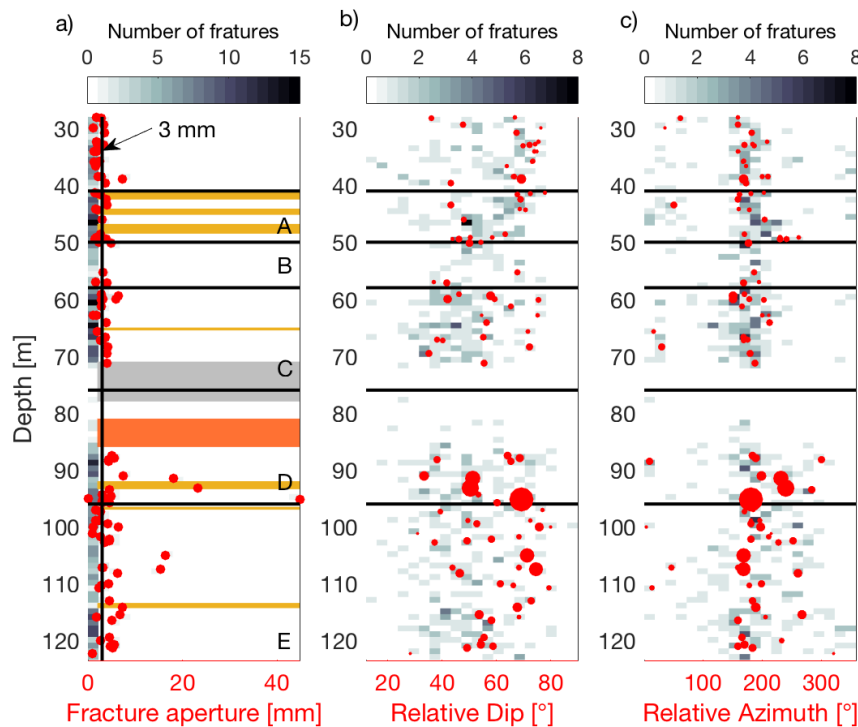


Figure 1: Summary of the brittle deformation based on the OTV data Egli et al. (2018) a) fracture aperture, b) relative dip and c) relative azimuth. All identified fractures are displayed in histographic form along the borehole. Fractures with measurable aperture (greater than 0.8 mm) are displayed as red dots. In a) additionally cataclastic zones, the cementation zone and main fault core are plotted.

**Comment 5:** The authors use the term borehole breakout to describe a zone intensely fractured. In literature borehole breakouts are an important indicator of horizontal stress orientation and are stress-induced enlargements of the wellbore cross-section (Bell and Gough, 1979) and occurs when the stresses around the borehole exceed that required to cause compressive failure of the borehole wall (Zoback et al., 1985; Bell, 1990). Here the term borehole breakouts is misleading, please change this term with enlargements, or similar.

**Author response and changes in the manuscript:** We agree with the referee that the term borehole breakout is misleading and we have therefore changed it to the more general term borehole enlargement throughout the manuscript.

**Comment 6:** Lines 97-99: Between 75 m and 95 m, there is a good match between the caliper (increasing), neutron-neutron (decreasing) and energy (decreasing) in the D zone, whereas the BHR shows a decreasing already at 70 m. How to explain this difference among the measurements?

**Author response:** The Caliper, neutron-neutron log and energy deficit are affected by the cemented borehole section. The latter two due to their relatively small penetration depth. Conversely, the BHR measurement has a significantly deeper penetration depth and is averaged over a larger support volume. Thus, the BHR measurement is likely to reflect the “true” formation properties better. Around this depth, the borehole collapsed during drilling due to intense brittle/cataclastic fracturing. The BHR data seem to reflect a transition towards the fault core here, which is not captured in the other measurements.

**Changes in the manuscript:** A corresponding comment was added in the manuscript.

**Comment 7:** Line 208: Does this mean that this interval is intact or more compact, and no fracture is present?

**Author response:** It is the section of the borehole with the lowest fracture density, but fractures are still present in the OTV, although they have apertures of less than 0.8 mm, which were deemed not to be reliably measurable for the recorded resolution of the OTV data.

**Changes in the manuscript:** A corresponding comment was added in the manuscript.

**Comment 8:** Line 412: It seems that these two zones, above and below 95 m, are hydraulically distinct. Is there a clay interval that separates the two reservoirs, or at least an aquiclude? Do you have some geological evidences?

**Author response:** There are three major fractures around 95 m, two above 95 m with apertures around 20 mm and one at 95 m with an aperture of 40 mm. Although, there is no clear geological evidence of an impermeable layer, below 95 m a zone of increased ductile deformation occurs, which seems to be more intact but still contains fractures with apertures of less than 3 mm. This is followed by a zone of weakly deformed granite, which may potentially act as a hydraulic barrier between the two hydraulically distinct “reservoir” zones. We are not aware of any other geological evidence.

**Changes in the manuscript:** The interpretation of two hydraulically distinct zones was added in the manuscript and is discussed in the extended discussion section.

**Comment 9:** Line 432: It means you have two separate water reservoirs. A shallow one, above 95 m where the meteoric water can penetrate into the formation through the fractures and change the salinity. Below 95 m a "deep" water reservoir with a different salinity content is present. What about the chemical composition of the water of both reservoirs? Are there any studies on the subject? Why are these two separated reservoirs, are there geological evidences of an aquiclude of an impermeable layer? what about the deep and shallow resistivity could you help you to identify the two reservoirs?

**Author response:** This is a plausible explanation of the data. However, we do not have the chemical composition of the water for the two potential reservoirs. A detailed analysis was only performed for the hydrothermal water entering the Transitgas tunnel below the borehole, which is published, for example, in Wanner et. al. (2019). The deep and shallow resistivity measurements are also not helpful here, as explained in 3.

**Changes in the manuscript:** Two potentially different water sources are now discussed in the discussion section as well.

**Comment 10:** Fig. 7: Why at around 46-49 mm, the ductile deformation intensity is high but the fractures/m curve indicates high number of fractures? Should not be this interval brittle?

**Author response:** The system consists of a ductile shear zone overprinted by brittle deformation. Wanner et al. (2019) for example state “The Breccia Fault is a product of brittle reactivation of an older ductile shear zone that belongs to the Grimsel Pass Fault Zone, a dense set of major ENE trending mylonitic faults that show late strike-slip displacement and that extend along strike over tens of kilometers through the Central Alps (Belgrano et al., 2016; Herwegh et al., 2017).” Furthermore, Egli et al. (2018) illustrated that the largest brittle deformation coincides with ductile deformation.

**Changes in the manuscript:** This is stated now in the section geological setting.

#### **Minor Comments:**

Reviewer comment, *Author response*

Line 197: Please delete one bracket

*Done*

Figure 4d on the left-hand shows only an interval related to a single area of cataclasite while in the text three areas of cataclasite are mentioned. Could you add the OTV images and core image boxes of the other two cataclasite zones as additional material?

*We added an image of the OTV data for the second cataclastic zone, however adding more OTV images of high quality will increase the size of the manuscript, without adding too much additional information.*

Line 208: Does this mean that this interval is intact or more compact, and no fracture is present?

*It is the section with the lowest fracture density, but fractures are still present in the OTV although they have small apertures less than 0.8 mm. Apertures below 0.8 mm were deemed not to be measurable for the recorded resolution of the OTV data. This was added in the manuscript.*

Line 212: Please add Fig4d (middle)

*Each subplot is labelled now and cited in the text.*

Line 214: please indicate in the Fig4d (middle) of OTV the fractures and please specify the aperture (mm) of the fractures.

*The position and the aperture of the fracture have been added in the manuscript. They are not in the interval of the OTV image.*

Line 222: please add the figure 4d right-hand.

*Each subplot is labelled now and cited in the text.*

Line 226: Were the resistivity measurements performed with the dual laterolog tool? If so, can you add the deep and shallow resistivity curves, including the ratio of depth to shallow, so as to highlight the invade zone or not?

*Please see the answer before (major comments).*

Line 231: please use enlargements, or similar instead of breakout.

*This was changed throughout the manuscript.*

Line 330: please add reference(s) Line

*A reference was added.*

Line 416: please specify the aperture of the fractures (mm) and how many fractures are characterized by large apertures

*All fracture apertures are now specified in Figure 5. Zone C: 9 fractures have an aperture above 3 mm and the largest aperture is 6.4 mm. Zone E: 16 fractures have an aperture above 3 mm and the largest aperture is 16.4 mm. This was added in the text.*

Line 421: Could you see this variation using the DLLdeep and DLLshallow and their ratio (deep/shallow)?

*See comment before.*

Line 435: A dot is missing after Fig. 12

*Done*

FIGURES: Fig 1. Please add the lithology and explain the the different colors along the borehole. Add a relative scale (zero on top of the borehole and the altitude at which the borehole is located).

The figure has been modified. The borehole is situated in a hydrothermally mineralized zone of the Southwest Aar granite. The main variation is the ductile deformation intensity.

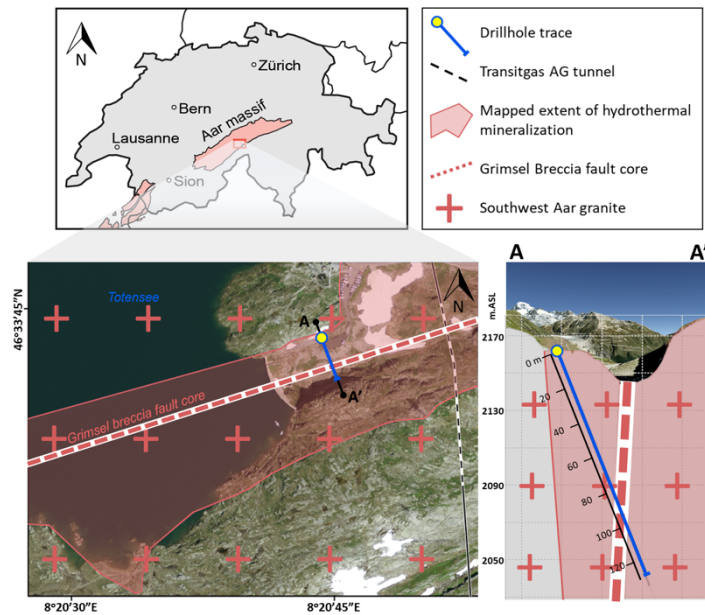


Figure 2. a) Aerial image (Source: Federal Office of Topography [www.swisstopo.ch](http://www.swisstopo.ch)) of the Grimsel Pass showing the trace of the GDP1 borehole, the extent of mineralized outcrops associated with the GBF (Belgrano et al., 2016), and the location of the Transitgas AG tunnel with the interval of active hydrothermal inflow marked by the white stippled line (modified from Egli et al. (2018)). b) Schematic crosssection through the plane of the borehole intersecting the GBF showing the extreme topographic relief in conjunction with the location and orientation of the borehole (modified from Greenwood et al. (2019)).

Fig 3. The blue circles around the red dots and squares are not visible. Please change. The figure is very small, I needed a large magnification to see the symbols and writings.

The figure has been changed to make the symbols more visible.

Fig. 4a,b,c: Please move the legend, it covers the energy deficit color scale and the data of Figure 4c. Add the meaning of the grey and orange bands. Please add on the legend the scale of the aperture of the fractures. Please add in the fig 4a both calipers (C1-3 and C2-4). This will allow the reader to see immediately if the whole interval is washout (e.g. C1-3 & C2-4) bit size) or breakout (eg. C1-3>C2-4 and vice versa). Insert in the figure caption the value of the bit-size of the borehole and also in the fig.4a, maybe as black dashed line.

The legend has been moved. The Caliper is a 3-arm caliper which has only one channel output.

Fig. 4d: The orientation of the OTV images is missing. Please add. I also suggest that you indicate structures such as fractures, bedding planes, etc. in the OTV images including the aperture of the fractures in mm. The OTV image refers to a longer interval than the core boxes. Please modify the figure. I also suggest that you provide a table that includes the fractures (depth, strike and dip) including the opening in mm (when it is possible). It is quite difficult to see these parameters (number of fractures, orientation and aperture) in the figure 4c

The figure has been modified and additional information has been added. A new figure (Fig 1 shown above) showing the fracture properties has been added.

Fig. 5: Please change the color of the titles caliper, P-wave velocity, , neutron-neutron, BHR and resistivity in green as the green curves. Please move the legend from the resistivity log.

The Color of the logs has been changed to correspond to the color of the titles.

Fig. 8: I like very much this figure, but the vectors of ECOP and DOP are very small. Please enlarge the figure.

*The Figure has been enlarged.*

## **References**

Belgrano, T. M., Herwegh, M., and Berger, A.: Inherited structural controls on fault geometry, architecture and hydrothermal activity: an example from Grimsel Pass, Switzerland, *Swiss Journal of Geosciences*, 109, 345–364, 2016.

Egli, D., Baumann, R., Küng, S., Berger, A., Baron, L., and Herwegh, M.: Structural characteristics, bulk porosity and evolution of an exhumed long-lived hydrothermal system, *Tectonophysics*, 747, 239–258, 2018.

Wanner, C., Diamond, L. W., and Alt-Epping, P.: Quantification of 3-D Thermal Anomalies From Surface Observations of an Orogenic Geothermal System (Grimsel Pass, Swiss Alps), *Journal of Geophysical Research: Solid Earth*, 124, 10 839–10 854, 2019.

**Table 3.** Petrophysical properties of the cluster groups (25th and 75th percentile) and core measurements

Cluster analysis	Cluster 1	Cluster 2	Cluster 3	Cluster 4	Drill core
Porosity [%]					0.84 - 14.73*
BHR	9 - 12	4.7 - 6.6	3 - 4	1.8 - 2.8	
Neutron-Neutron	10 - 16	4.5 - 6.9	2.8 - 3.5	2 - 2.5	
	(max: 26)	(max: 12.2)		(min: 1.6)	
P-wave velocity [m/s]	2920 - 3377	3548 - 3849	4056 - 4482	4464 - 5013	5386 - 5861**
	(min: 2613)			(max: 5603)	(4657 - 5448)
S-wave velocity [m/s]	1878 - 2225	2135 - 2352	2347 - 2549	2523 - 2744	2952 - 3380**
	(min: 1732)			(max: 3024)	
Rock type	Fault breccia	Cataclasite	Mylonite/Ultramylonite	Gneiss	Granite
Mean matrix and micro-fracture porosity*** [%]	14.8	10.8	3 - 4	2.3	0.9

\*personal communication Jörg Renner,\*\* Ultrasonic measurements for saturated (and dry) samples under ambient conditions (personal communication Jörg Renner), \*\*\* Egli et al. (2018) Multi-scale analysis

## 6 Discussion

The BHR reflection image reveals a network of fluid-filled fractures in the damage zones above and below the main fault core. A projection of the reflections identified in this image onto the borehole track is shown in Fig. 13. Reflections with relative dips above 55° are well captured by the image and in good agreement with the interpretation of the OTV data. Conversely, events with smaller dips are more difficult to detect due to the single-hole setup and the limited offset. The extent and continuity of reflections away from the borehole can only be assessed in zones with low signal attenuation, as evidenced by high first-cycle amplitudes. **In these zones, fractures can be tracked up to 5 m into the formation revealing an interconnected fracture network.** High signal attenuation, as evidenced by low first-cycle amplitudes, occurs in several zones characterized by intense brittle deformation. This also prevents a more quantitative analysis of the reflection amplitudes, which could be theoretically related to fracture apertures in a more favorable environment.

Although there are uncertainties in the absolute values of the measurements due to borehole enlargements, the relative variations of the petrophysical properties are clearly dominated by the different degrees of brittle deformation. Table 3 summarizes the range (25th and 75th percentiles of the median) of porosity, P- and S-wave velocities for the groups identified in the cluster analysis and compares them to core measurements and average matrix and micro-fracture porosity estimates of Egli et al. (2018). These authors differentiate matrix porosity types by their mineralogy and texture: quartz dominated zones are governed by inter- and intragranular porosity (0.8%), feldspar dominated areas by solution porosity (1.4%), fine-grained mica (75 μm) and coarse grained mica by inter- and intragranular porosity (2.8% and 4.6%), whereas breccia porosity is significantly higher. A summary of their estimates for mean matrix and fracture porosity is provided in Table 3. These estimates obviously do not

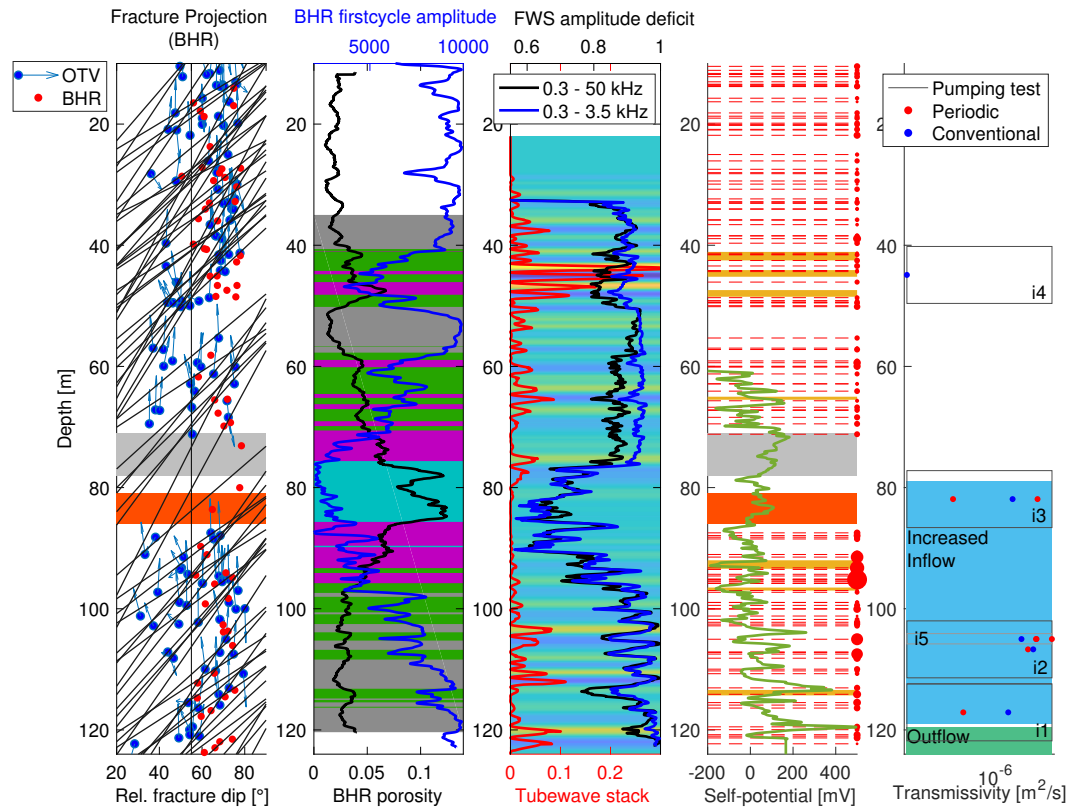


**Figure 13.** From left to right: Projection of imaged BHR reflections onto the borehole track together with associated dip, tadpoles illustrating the azimuth and dip for the fractures identified from the OTV data; results of cluster analysis overlain by BHR porosity and BHR amplitudes; tubewave stack overlain by tube wave energy (Greenwood et al., 2019) and Stoneley energy deficit; brittle deformation data overlain by the corrected SP log (2017); and summary of transmissivities estimated from pumping tests (Cheng and Renner, 2017).

account for larger fractures, which are captured by the log data. Nevertheless, for the cataclasites and the fault breccia the mean porosity estimates fall within the range of values obtained for clusters 1 and 2, which are categorized as the main fault core and regions of high fracture density or cataclastic zones, respectively. The values for clusters 3 and 4, which cover sections of the borehole with moderate to low fracture density, are quite similar to mean matrix and micro-fracture porosity values of the granites, gneisses and mylonites. However, a more detailed differentiation between these tectonic groups based on the log data is not possible. Ultrasonic velocity measurements performed on selected core samples generally provide higher values than the sonic log measurements. However, the maximum velocity values of the sonic log data in cluster 4, which comprises the most intact rocks, fall within the range of these laboratory measurements. The chosen core samples cover different types of fabric variations (granitoids, gneiss and mylonites) and are from the more intact parts of the recovered drill core. Nevertheless, even these core samples still seem to contain fractures, as evidenced by the non-negligible difference between dry and saturated

ultrasonic P-wave velocity measurements. This suggests that the elastic response of the damage zone of the GBF is dominated by the mechanical compliance of fractures at multiple scales.

490 The energy deficit of the Stoneley wave is related to the hydraulic transmissivity. At lower frequencies, this wave type is referred to as a tube wave and commonly encountered in hydrophone VSP surveys. Greenwood et al. (2019) linked the tube waves along the GDP1 borehole to hydraulically open fractures. Figure 12 compares the tube wave energy along the borehole with the energy deficit of the low-frequency FWS data. Both measures respond to hydraulically open fractures along the borehole. For the cataclastic zones and some of the large-scale fractures, we observe a good correlation between the two energy  
495 measures. In the zone around the main fault core, the agreement is less good, since borehole enlargements and the rugosity of the borehole wall prevent the propagation of tube waves. However, tube waves are still created in this region as shown by Greenwood et al. (2019). Thus suggesting that these are zones/features of increased hydraulic transmissivity. Furthermore, the distinct anomalies of the wave energy deficit in the damage zone below the GBF show a very good correlation to the anomalies encountered in the SP data. This supports our interpretation that the SP anomalies are related to fluid flow governed by  
500 hydraulically open fractures.

For specifically targeted zones, indicated in Fig. 13, Cheng and Renner (2017) performed conventional and periodic pumping tests in the GDP1 borehole in 2015. The resulting transmissivity estimates are shown in Fig. 13. The highest values are obtained for the intervals i2 and i5, which feature a large aperture fracture of 16.4 mm at 105 m borehole depth. This fracture  
505 can be associated with a distinct anomaly in the SP data and the energy deficit. However, no clear trend can be established between the magnitude of the anomalies in the two log attributes and the estimated transmissivity from the pumping tests. One reason is that the pumping test only provides a few values of transmissivity averaged over relatively large intervals. The logs analyzed in this study do, however, point to a compartmentalized system with distinct hydraulic zones with water of different origins. A hypothesis is the existence of a shallow water reservoir above 95 m depth where meteoric water penetrates into the  
510 formation through the exposed fracture network, whereas below 95 m depth, a deeper and more saline hydrothermal water reservoir may prevail. Eventhough there is no clear evidence of a hydraulic barrier between the two zones, below 95 m depth, a zone of increased ductile deformation with fracture apertures smaller than 3 mm followed by a zone of weakly deformed granite may act as such a barrier. Furthermore, the results of Cheng and Renner (2017) suggest a complex and variable flow geometry on the decameter scale in the studied subsurface region of the GBF associated with a heterogeneous system dominated  
515 by steeply dipping structures with a pipe-like hydraulic behavior. No chemical analysis of the water in the GDP1 borehole was conducted. However, the interpretation of different water sources is consistent with the recent hydrogeochemical study of Wanner et al. (2019) carried out in the Transitgas AG tunnel situated 200 m below the GDP1 borehole. The study identified two types of springs along the tunnel: i) cold springs with a low mineralization (total dissolved solids (TDS) < 100 mg/L) and (ii) warm springs with elevated mineralization (TDS > 250 mg/L). The composition of the warm springs can be well explained by  
520 a binary mixture between a geothermal component characterised by elevated salinity and temperature and weakly mineralized

cold meteoric water from the surface.

525 All of this points to the presence of distinctively different sources and passages of fluid flow in the studied subsurface region of the GBF (GDP1 borehole), thus suggesting a compartmentalization of fluid pathways in the hydraulic system along steeply dipping intersecting fractures and cataclastic zones. The main flow paths are associated with the intensely fractured nature of the exhumed ductile shear zone. Fracture permeability is expected to decrease with depth due to its inherent pressure-dependence, but cataclastic zones may retain a part of their porosity due to hydrothermal processes. Furthermore, Egli et al. (2018) suggested that fault intersections act as regions of high permeability in the Grimsel Pass hydrothermal zones. These intersections inferred from the drill hole data and observed in the BHR data may prevail on a larger scale along the GBF, effectively feeding a hydrothermal reservoir with meteoric water and allowing localized up-flow of hydrothermal water along cataclastic zones (subsidiary fault cores) and fault intersections (Egli et al. (2018). This interpretation is supported by the study of Belgrano et al. (2016), which analyzed the architecture and hydrothermal activity of the GBF on a larger scale and concluded that the hydraulic characteristics are controlled by localized sub-vertically oriented pipe-like upflow zones. Furthermore, a recent study of Wanner et al. (2019) based on 3D thermal-hydraulic modelling constrained by surface observations of warm springs and fossil hydrothermal mineralization, suggested that the thermal anomaly at the Grimsel Pass may reach down to 9 km depth. They did, however, argue that, this specific anomaly is not a suitable candidate for petrothermal power production due to its comparatively low flow rates.

530

535